Desalination and Water Treatment
www.deswater.com
doi: 10.1080/19443994.2015.1036467

57 (2016) 10286–10294
May

Taylor & Francis
Taylor & Francis Group

Optimization of horizontal photocatalytic reactor for decolorization of methylene blue in water

Khatcharin Wetchakun[a,*], Natda Wetchakun[b], Sukon Phanichphant[c]

[a]*Faculty of Science, Program of Physics, Ubon Ratchathani Rajabhat University, Ubon Ratchathani 34000, Thailand, Tel. +66 82 631 1130; Fax: +66 45 352 070; email: khatcharin@gmail.com*
[b]*Faculty of Science, Department of Physics and Materials Science, Chiang Mai University, Chiang Mai 50200, Thailand*
[c]*Faculty of Science, Materials Science Research Center, Chiang Mai University, Chiang Mai 50200, Thailand*

Received 1 December 2014; Accepted 25 March 2015

ABSTRACT

The prototype photocatalytic reactor was designed and then constructed in a horizontal scheme for testing the decolorization of methylene blue (MB) as a toxic organic model by UVA irradiation. The optimization of the photocatalytic reactor with a recycling system using TiO_2 nanoparticles (P25) as photocatalysts was investigated in this work. The efficiencies on MB photocatalytic decolorization of three geometric photocollectors in the reactor: (i) parabolic through collector (PTC), (ii) compound parabolic collector (CPC), and (iii) flat-plate collector (FPC), including the presence and the absence of parabolic reflector cover the UVA tubular lamp as an artificial light source were compared. Excepting only the CPC, the experimental results indicate that the orientation of light rays using the reflector as a primary and the collector as a secondary, can improve on the photocatalytic efficiency of MB decolorization. In our case, the PTC with the presence of the reflector shows higher performance on the MB decolorization than the CPC with the absence of the reflector and the FPC with the presence of the reflector. The photocatalytic reaction over MB decolorization can be explained under pseudo-first-order kinetics model. For our study, the optimums of MB suspension flow rate and TiO_2 catalyst concentration were found toward 345 mL/min and 1.0 g/L, respectively.

Keywords: Decolorization; Methylene blue; Photocatalytic reactor; Titanium dioxide

1. Introduction

Thailand as a country has been confronting with the problems of water management and water treatment. Until now, the methodologies and technologies used for solving the problem have been unsustainable. In many countries, heterogeneous photocatalysis in advanced oxidation technology has been selected and pushed to build solar photoreactor in pilot plant for treating wastewater. In previous works, photocatalytic reactors under UV/visible/solar irradiation were designed in many shapes such as parabolic through reactors, compound parabolic collecting reactors (CPCRs), flat-plate reactors [1–3], etc. For the most of photocatalytic researches, the slurry system using photocatalyst particles suspended in water is preferred to the fixed or supported catalyst system, even though the slurry system needs the requirement of the catalyst separation step. This is because the slurry system

*Corresponding author.

shows higher water treatment performance than the other (approximately five times) [4,5]. Commercial TiO_2 (P25) as a semiconductor nanophotocatalyst, containing around 85% of anatase and 15% of rutile, has been accepted that it exhibits high power photocatalytic activity, responding with UV–vis light [6]. Nowadays, P25-TiO_2 is largely used in industrial plants due to its worldwide markets and excellent catalytic properties. Although new photocatalyst materials have been discovering, they cannot be successfully brought into global markets with a number of limitations. Likewise, Di Paola et al. [7] revealed that alternative materials suitably represented TiO_2 on photocatalytic detoxification have not been found.

Some countries located on the equator have an advantage of using full benefits from solar energy. Generally, the construction of solar reactors is tested their alignments (east–west or north–south) and tilted to an angle of city latitude for optimizing their applications [8–10]. In the past region, testing on photocatalytic reactor performance toward water treatment application was classified into two methods as follows: (i) mathematical simulations and (ii) actual experiments. Moreover, photoreactor system was divided into two styles: (i) stirring and (ii) continuous flowing. However, the continuous flowing system has been used in pilot scale due to its large volume supporting. The photoreactor test via experiment method under continuous flowing system has still needed the studies toward many parameters affecting the efficiency of the photocatalytic reactions. Moreover, there are insufficiently many works focused on developments about photocatalytic reactor design and system to satisfy sustainable applications. For example, in 2004, Bandala et al. [11] showed the effect of different collector shapes on the efficiency of solar heterogeneous photocatalytic decomposition of oxalic acid in water. The results showed that the CPCR presented the best overall performance. However, the photoreactor designed on various managements of light rays by adding a parabolic reflector cover the UVA lamp as an artificial light source with different collector shapes through the discussion of its photocatalytic performance on methylene blue (MB) decolorization was not published.

Therefore, this work is focused on studying and comparing the photocatalytic efficiencies over the decolorization of MB used as a toxic organic model toward the different arrangements inside the prototype photoreactor. The aim of this research is to discover the optimum of the prototype photocatalytic reactor with varying two photocatalytic factors: catalyst concentration and MB suspension flow rate, and with varying six arrangements of the geometric photocollectors: (i) parabolic through collector (PTC), (ii) compound parabolic collector (CPC), and flat-plate collector (FPC), including the presence and the absence of the parabolic reflector for all collectors.

2. Materials and methods

2.1. Materials

The toxic cationic dye, methylene blue ($C_{16}H_{18}N_3ClS$, λ_{max} = 665 nm) from Sigma-Aldrich, Australia, was selected to be an organic dye model which was dissolved in deionized water (RCI Labscan, Thailand) for testing the photodecolorization with the prototype photocatalytic reactor. Commercial titanium (IV) oxide, Aeroxide® P25 from Aldrich, Germany, was used as a photocatalyst for all testing. (≥99.5% trace metals basis; particle size: 21 nm (TEM); and surface area: 35–65 m^2/g).

2.2. Prototype photocatalytic reactor

The photocatalytic reactor was designed and then constructed as a prototype. A 10-W black light fluorescent lamp (F01T8 BLB), Santory, Japan, was used as a UVA light source for exciting the catalyst. The lamp was set in upper square aluminum box (grade 1100). The dimensions of the aluminum box are 28 cm wide × 28 cm long × 28 cm high. Three geometric photocollectors (PTC, FPC, and CPC), with and without the parabolic reflector covered over the tubular lamp, were put in the lower aluminum box for testing the MB photodecolorization to find out its optimal configuration. The photoreflector and photocollectors were also made from aluminum sheets (grade 1100) with their thickness of 0.3 mm. The borosilicate glass reactor tube of 40 mm in diameter and 155 mm in length was aligned in horizontal direction and was parallel to the tubular lamp with the distance between them of 14 cm. A 250-mL reservoir tank was connected to the peristaltic pump (BT101S, Lead Fluid, China) for providing and receiving the aqueous MB suspensions. The flow rates of the MB suspension were varied as follows: 230, 345, 460, and 575 mL/min. The schematic model of the prototype photocatalytic reactor in laboratory scale for decolorizing MB is shown in Fig. 1.

2.3. Photocatalytic testing and analyzing from using the prototype reactor with 10-W UVA lamp as a light source

The performance of the photocatalytic reactor was evaluated by testing the decolorization of MB under UVA irradiation and dark condition in close system at

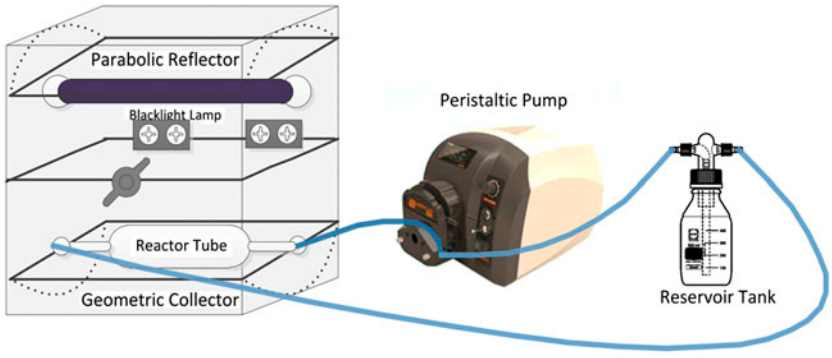

Fig. 1. Schematic representation of photocatalytic reactor with continuous flowing system.

24°C of room temperature. MB solution in 250 mL with the initial concentration (C_0) of 17 mg/L was prepared. Amounts of P25-TiO_2 catalyst are varied in the range of 0–2 g/L. The MB volume of 250 mL is suitably fixed on the flowing system of the photoreactor. The MB solution was mixed with the catalyst nanopowders under natural pH. Prior to UVA irradiation, the suspension was kept under dark condition for 30 min to achieve adsorption–desorption equilibrium. Under UVA irradiation, the MB suspension of 6 mL was collected every 15 min until at the irradiation time of 30 min and every 30 min until at the irradiation time of 240 min. The MB sample at that time was centrifuged at 13,000 rpm by a microcentrifuge machine (ScanSpeed, Labogene, Denmark) for 5 min twice times. The plastic Pasteur pipette was used for transferring MB solution for protecting the absorption of MB on the pipette surface. Absorbance of all MB samples was analyzed by T90+ PG Instruments spectrophotometer at 613 nm which corresponds to a characteristic absorption peak of MB, and then was converted into the MB concentration (C) at that time by using Beer–Lambert's law, since the absorption band at 665 nm shifted to the blue region from generating some intermediates [12]. The UVA light intensities at the middle bottom surface of the reactor tube were measured by using TM-208 UVA light meter, Tenmars, Taiwan.

3. Results and discussion

3.1. The design of prototype photocatalytic reactor

The PTC and CPC were designed following the details as shown in Table 1: the PTC and CPC design parameters. On the CPC design, two parabolas were tilted oppositely away from vertical axis with the angle (θ_a) of 16°, having the focus point of the tiled parabolas in 7 cm, and k value of 0 cm (at y axis) matching with h values of 2 cm and −2 cm (at x axis). The length in the range of h values fits well with the diameter of the reactor tube. The PTC and CPC were laid on horizontal direction inside the aluminum box. Fig. 2 shows the calculated curves of the PTC and CPC. The CPC curve in Fig. 2(b) was used only the internal trend points on both of sides. The

Table 1
Main characteristic parameters of the PTC and CPC

Parameter	PTC	CPC
Equation	$y^2 = 4fx$	$x' = (y-k)\sin\phi + (x-h)\cos\phi$ $y' = (y-k)\cos\phi - (x-h)\sin\phi$ by $y^2 = 4fx$ and h = 2 cm, k = 0 cm
Mounting	Horizontal axis	Horizontal axis
Semi-acceptance angle, θ_a*	–	16
Focus length (cm)	7	7
Aperture area (cm^2)	660.8	613.2
Concentration ratio, C_{CPC}*	–	3.64
Concentration factor, R_C*	–	3.03
Photoreactor OD (cm)	4	4
Photoreactor ID (cm)	3	3

*The parameters are only used for CPC.

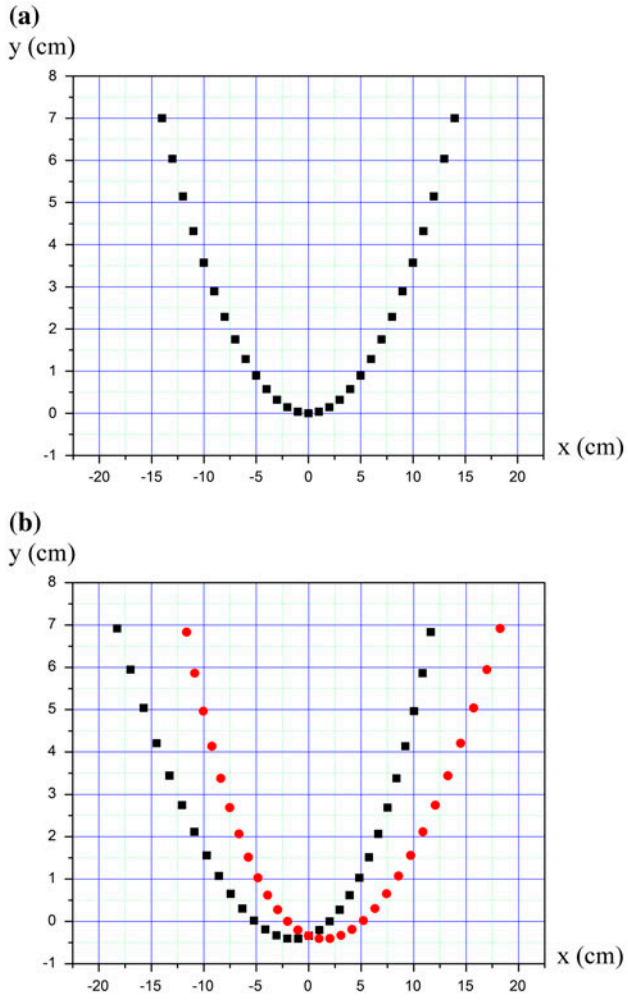

Fig. 2. Curve plotting of the (a) PTC and (b) CPC with a semi-angle of acceptance (θ_a) of 16° at the focus point of 7 cm.

concentration factor (R_C) and the concentration ratio (C_{CPC}) of the CPC in two dimensional are given as $R_C = 1/\sin(\theta_a/2)$ andC_{CPC} = aperature area/absorber area, respectively, where θ_a is semi-acceptance angle. The parabolic reflector covered over the lamp was designed following the PTC.

3.2. Effect of collector shapes on the methylene blue photodecolorization

The performance of the photocatalytic reactor, comprising of with different photocollectors inside the photoreactor box as follows: PTC, CPC, and FPC, including the presence and the absence of the parabolic reflector cover the lamp (using the code of "pr-" and "npr-", respectively, laid before the abbreviation of the name of all collectors) on MB decolorization, is shown in Fig. 3. The MB decolorization performance of the photoreactor with different conditions was examined on the photocatalytic decolorization rate using UV–vis spectroscopy technique. Mostly, Langmuir–Hinshelwood (L–H) model has been successfully fitted to the kinetics of the MB decolorization in heterogeneous photocatalytic activity [13]. The equation is as follows:

$$R = -\frac{dC}{dt} = k_r\theta = k_rKC(1+KC) \quad (1)$$

where R is the photocatalytic reaction rate, C is the concentration of MB, t is the reaction time, k_r is the reaction rate constant, θ is the fractional site coverage by MB, and K is the MB adsorption coefficient. The result of the integration of Eq. (1) is corresponding to the first-order rate model by having the negative interception value:

$$\ln\left(\frac{C}{C_0}\right) = -k_{app}t - K(C - C_0) \quad (2)$$

where C_0 is the initial concentration of MB, C is the rest concentration of MB at that UVA irradiation time, and k_{app} is the apparent rate constant from determining the initial MB concentration. In Fig. 3, the reaction rates of the MB photodecolorization can be fitted well with the apparent first-order rate law according to Eq. (2). The linear trend of the relationship between ln (C/C_0) and irradiation time was found in two stages. The apparent

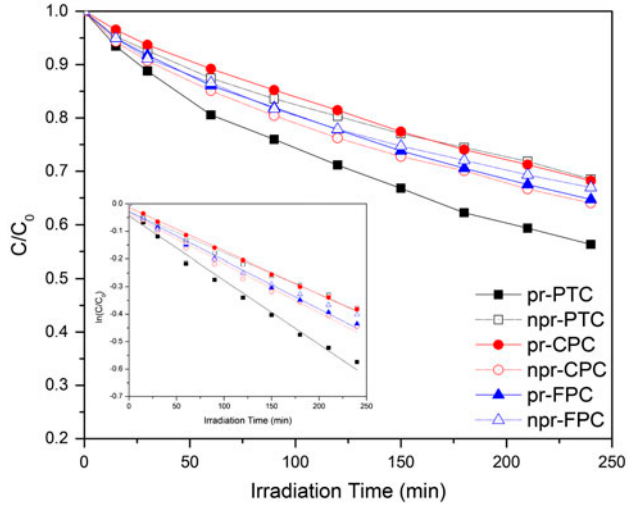

Fig. 3. Plotting of C/C_0 vs. UVA irradiation time using P25-TiO_2 as a photocatalyst at the suspension flow rate of 460 mL/min in different photocollector arrangements. Inset shows linear fitting between ln (C/C_0) and time.

rate constant in the first stage (0–30 min) is quite more than that in the second stage (60–240 min). This is expected to the effect of the MB adsorption kinetics for the first stage [14].

For the PTC and FPC, the presence of the parabolic reflector cover the lamp shows higher efficiency significantly for decolorizing MB than the absence of the parabolic reflector cover the lamp. This may be because the light rays coming from the original source without the reflector have large spreadability and can be poor captured by the PTC and FPC. Conversely, the npr-CPC reveals the ability in capturing the scattering light rays in all directions better than them. However, the npr-CPC shows the similar and lower rate constants of the MB photodecolorization reaction to pr-FPC and pr-PTC, respectively (Table 2). This can be expected that the orientation of the light rays from the reflector through the reaction tube is significant than that from the collectors, excepting in the case of the CPC. The apparent first-order rate constants following the photocollector arrangements from the highest one to the lowest one are ranked in order as follows: pr-PTC, npr-CPC, pr-FPC, npr-FPC, pr-CPC, and npr-PTC.

These results may be relating to both of factors as follows: the light flux from their light capturing abilities (F_{cap}) and the light intensity from their light concentrating abilities (F_{con}). The relative equation could be shown as $R \propto [F_{con}]^m [F_{cap}]^n$, where m and n are the constants. On the measurement of light intensities at the point of the middle bottom wall of the reactor tube for all collectors, they are around 28 and 40 $\mu W/cm^2$ toward the absence and the presence of the photoreflector, respectively. It is mean that for the PTC and the FPC, the light concentrating ability shows more influence than the light capturing ability for decolorizing MB.

The results exhibit correspondence with many previous researches reporting that under solar radiation, CPC were more efficient than PTC without any reflectors for arranging primary light rays before reaching to the reactor [11,15–19]. Therefore, it is a critical point to many incoming related researches focused on the increase in water treatment efficiency. However, for our study case in using a black light fluorescent lamp (artificial radiation), the efficiency of the pr-PTC on the MB decolorization is better than that of the npr-CPC. For applying to pilot scale, although under solar radiation according to the zenith angle, the diffuse radiation can be similar to the direct radiation on a clear sky day. On this consideration, it can be modified and applied to solar reactor for improving its performance, especially the countries around the equator. Moreover, the results can help in designing photocatalytic reactors for the future in the laboratory scale.

From considering the kinetics of the MB photocatalytic decolorization, they were compared with previous researches revealed as a pseudo-first-order rate law, as shown in Table 3. In Table 3, the apparent first-order rate constants of the MB photodecolorization reaction are in the range of 8.25×10^{-2}–5.34×10^{-4} min^{-1} which actually depends on particular light intensities, initial MB concentrations, catalyst concentrations, and adjusted pH values.

3.3. Effect of fluid flow rate on methylene blue photodecolorization

Effect of the suspension flow rate on the MB photodecolorization was investigated in the term of the ratio of C/C_0 vs. reaction time as shown in Fig. 4(a). The trend of the MB decolorization rate increases as the trend of fluid flow rate from 230 to 345 mL/min. When the flow rate values are higher than 345 mL/min, the trend of the MB photodecolorization rate reaches to the constant state (Fig. 4(b)). Therefore, the result shows the optimal flow rate of 345 mL/min (the critical limited value) along horizontal alignment of the reactor tube using amount of P25-TiO_2 at 0.5 g/L. It is expected that the increase in flow rate can help in improvement of the photochemical interactions since higher kinetic energy of the suspension affects to the increase in the energy in exchanging electrons and hydroxyl ions

Table 2
Photocollector arrangement-dependent kinetics of the MB photodecolorization

Photocollector arrangement	Apparent first-order rate constant, k_{app} (min^{-1})	R^2
pr-PTC	2.33×10^{-3}	0.98403
npr-PTC	1.49×10^{-3}	0.98628
pr-CPC	1.57×10^{-3}	0.99694
npr-CPC	1.78×10^{-3}	0.98273
pr-FPC	1.76×10^{-3}	0.99004
npr-FPC	1.62×10^{-3}	0.97922

Table 3
Summary of photocatalytic decolorization of methylene blue (MB) using TiO_2 as a photocatalyst

References	Catalyst type and concentration	Light source and intensity	pH value and MB volume	Concentration of MB	Pseudo-first-order kinetic constants (min^{-1})
Zhang et al. [12]	Degussa P25 of 100 mg; 2 g/L	75 W Hg lamp; 3.6 mW/cm^2	pH 3.85; 50 mL	0.3 mM/ 12.79 mg/L	$1.5 \pm 0.4 \times 10^{-2}$
Byun and Kwak [20]	TiO_2	UV irradiation	50 mL	0.14 mM	0.0825
Mohapatra and Parida [21]	Sulfate-modified TiO_2; 1.6 g/L	6-W low-pressure Hg vapor lamp (90% of light at 254 nm);	25 mL	100 ppm	0.00783
Mohamed and Al-Esaimi [22]	Vanadium-doped TiO_2 and sulfated TiO_2 (rutile); 1 g/L	100-W Hg lamp (output mainly at 400 nm, Toshiba SHLS-1002 A); 125 W/m^2	100 mL	50 mg/L	0.037 (2 V/TiO_2–SO_4) 0.030 (2 V/TiO_2)
Senthilkumaar et al. [23]	Sol–gel derived silver-doped nanocrystalline TiO_2; 0.533 g/L	125-W (311 nm) medium-pressure Hg arc lamp; 1.6×10^{-4} Einstein/min	pH 6.80; 150 mL	10 mg/L	0.03147
Kim et al. [24]	TiO_2 nanoparticles; 0.3 g/L	9-W black light blue lamp (Philips, PLS9 W/08.BLB)	1,000 mL	0.5 mM	1.5128×10^{-3}
Abdullah and Chong [25]	Tungsten-loaded TiO_2; 1 g/L	250-W metal halide lamp (Venture Lighting, USA); 21,000 lx	pH 6; 100 mL	40 ppm	0.028
Kang and Chen [26]	TiO_2 nanotube arrays; 1 cm × 1 cm	UV lights (365 nm, 6 W)	N/A	26 μM	0.0242 (500°C)
Acosta-Silva et al. [27]	7–31% TiO_2/SBA-15	125-W medium-pressure mercury lamp	100 mL	40 mg/L	0.0136 (31% TiO_2/SBA15) 0.0026 (Degussa P25)
Boiarkina et al. [28]	TiO_2-coated glass disk	Low-pressure mercury UV lamp inside a quartz tube (20 W); 12–23 W/m^2	550 mL	10 mg/L	5.34×10^{-4}
Kasanen et al. [29]	Multilayer TiO_2 coating on HDPE with PU binder dilution 1:8	A high-intensity UV lamp (UVP Black Ray B100AP, Upland, CA); far from MB solution of 82 mm	pH 7.64	3.2 mg/L	7.1667×10^{-3}
Ahmed [30]	Mesoporous NiO/TiO_2 nanocomposites; 1 g/L	High-pressure mercury lamp with maximum absorption at 254 nm	100 mL	10^{-5} mg/L	0.0133 (pure TiO_2) 0.019 (NiO/TiO_2 nanocomposite)
Sahoo et al. [31]	Silver ion-doped TiO_2; 2 g/L	15-W lamp from Phillips emitting UV light of wavelength 254 nm; far from MB solution of 10.5 cm	pH 6.8; 60 mL	20 ppm	0.0168 (TiO_2) 0.0273(Ag^+ doped TiO_2)
Abdelaal and Mohamed [32]	TiO_2 nanocomposite prepared by modified sol–gel method; 1.5 g/L	Xenon lamp (300 W) doubly covered with a UV cut filter; 0.1 mW/cm^2	500 mL	100 mg/L	10×10^{-4} (TiO_2) 40×10^{-4} (Pd/TiO_2) 80×10^{-4} (TiO_2–Composite) 140×10^{-4} (Pd/TiO_2– Composite)

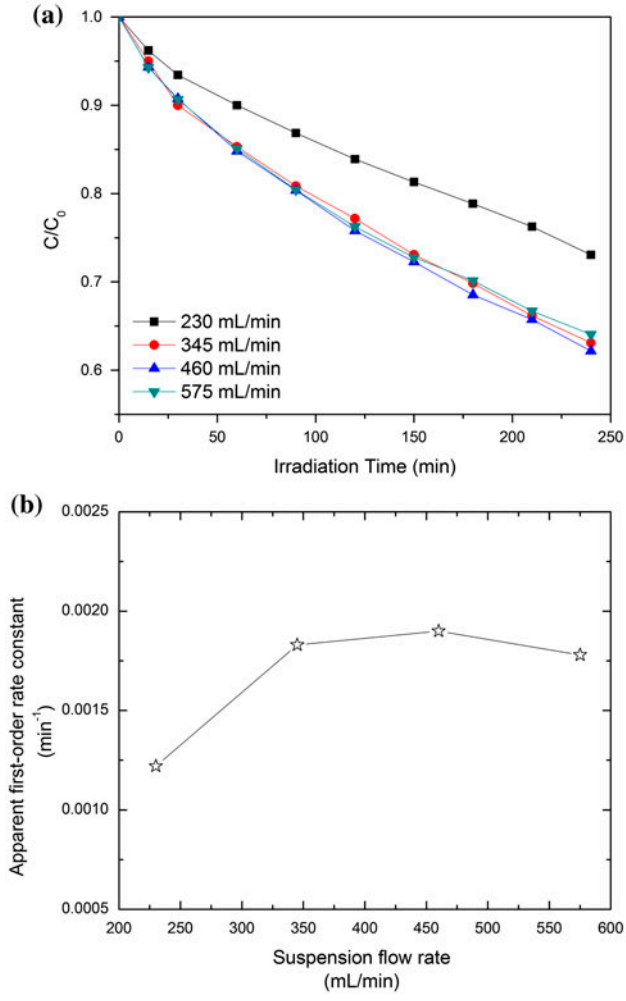

Fig. 4. Effect of flow rates of the suspensions on the MB photodecolorization reaction at the constant P25-TiO_2 concentration of 0.5 g/L as the functions of (a) C/C_0 vs. UVA irradiation time and (b) the apparent first-order constant vs. suspension flow rate.

between active sites of the catalyst and MB molecules. Moreover, the increase in flow rate creates the turbulence in fluid flow, so this can also help in the dispersion of the catalyst in the solution [33]. The optimal value of flow rate of the suspension depends on reactor size and alignment of the reactor tube. These are different with previous researches studying photoreactors in continuous flowing systems [34,35] due to the characteristic of the system.

3.4. Effect of P25-TiO_2 concentration on methylene blue photodecolorization

Fig. 5 shows the rate of the MB photodecolorization using P25-TiO_2 catalyst with its different concentrations under UVA irradiation and dark condition.

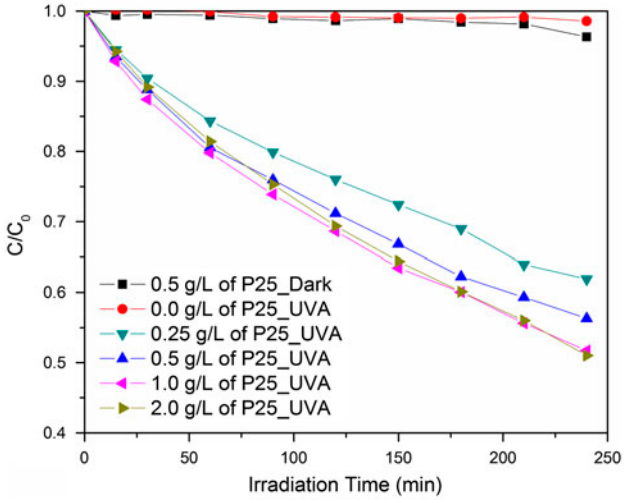

Fig. 5. Effect of P25-TiO_2 concentrations in the range of 0–2 g/L on the MB photodecolorization reaction at the suspension flow rate of 460 mL/min using the pr-PTC as a function of C/C_0 vs. reaction time.

The efficiencies of the MB photodecolorization increase as the increase in amounts of P25-TiO_2 photocatalyst from 0 to 0.5 g/L and then tend to be similar following the increase in amounts of P25-TiO_2 photocatalyst from 1.0 to 2.0 g/L. The tendency can be explained that when all cationic dye molecules are sufficiently adsorbed on the photocatalyst surface, there is no more area for active sites on the photocatalyst surface to make more photocatalytic reactions for decolorizing MB in water. Moreover, a number of photocatalyst particles dispersing in water can block light rays. Consequently, the optimal catalyst concentration for decolorizing MB in our case study was found to be 1 g/L of P25-TiO_2 at the constant suspension flow rate of 460 mL/min using the pr-PTC. From the previous literatures on the investigation of photocatalytic water treatment in continuous flowing system, the catalyst concentrations were mostly used in the range of 0.04–0.5 g/L and not more than 2.0 g/L, as shown in Table 3 and other researches [36–47]. The optimum of P25-TiO_2 concentrations possibly depends on the suspension flow rate used in the independent system for purifying water.

4. Conclusions

The inner structures of the photocatalytic reactor with different arrangements were compared for discovering its optimization. The results reveal the interest of the presence and the absence of the parabolic reflector cover the tubular lamp toward different

geometric collectors relating to their abilities of light capturing and light concentrating through the reactor tube. The PTC with the parabolic reflector provides the highest MB decolorization rate. On the other hand, in the case of the absence of the parabolic reflector over the lamp, the CPC shows the best efficiency in decolorization of MB. The different photocollector arrangements following the MB decolorization rate from the highest one to the lowest one are ranked in order as follows: pr-PTC, npr-CPC, pr-FPC, npr-FPC, pr-CPC, and npr-PTC. Based on this study, the optimization of the photocatalytic reactor reveals the configuration of its inner structure of pr-PTC with the suspension flow rate of 345 mL/min and P25-TiO_2 concentration of 1.0 g/L. The research results can help in improving the performance of photocatalytic activity for upcoming researches in laboratory scale with the photocatalytic reactor design having the prominent point in saving energy. For full-scale application, the economic and geographic evaluation for constructing the photocatalytic reactor using solar light in pilot scale to treat wastewater will be required on future research project.

Acknowledgments

The authors gratefully acknowledge financial support from Ubon Ratchathani Rajabhat University (Project Grant Number 95476) and the Centre of Excellence in Materials Science, Chiang Mai University. We also acknowledge the National Research Council of Thailand and Program of Physics, Faculty of Science, Ubon Ratchathani Rajabhat University for providing all supports. The National Research University Project under Thailand's Office of the Higher Education Commission and Chiang Mai University, Thailand, are also acknowledged.

References

[1] O. Alfano, D. Bahnemann, A. Cassano, R. Dillert, R. Goslich, Photocatalysis in water environments using artificial and solar light, Catal. Today 58 (2000) 199–230.
[2] S.P. Kamble, S.P. Deosarkar, S.B. Sawant, J.A. Moulijn, V.G. Pangarkar, Photocatalytic degradation of 2, 4-dichlorophenoxyacetic acid using concentrated solar radiation: Batch and continuous operation, Ind. Eng. Chem. Res. 43 (2004) 8178–8187.
[3] A. Fernández-García, E. Zarza, L. Valenzuela, M. Pérez, Parabolic-trough solar collectors and their applications, Renewable Sustainable Energy Rev. 14 (2010) 1695–1721.
[4] R.L. Pozzo, M.A. Baltanás, A.E. Cassano, Towards a precise assessment of the performance of supported photocatalysts for water detoxification processes, Catal. Today 54 (1999) 143–157.
[5] M.K.-e. Bouchareb, M. Bouhelassa, M. Berkani, Optimization of photocatalytic decolorization of C.I. Basic Blue 41 in semi-pilot scale prototype solar photoreactor, J. Chem. Technol. Biotechnol. 89 (2014) 1211–1218.
[6] M.I. Litter, Heterogeneous photocatalysis transition metal ions in photocatalytic systems, Appl. Catal., B 23 (1999) 89–114.
[7] A. Di Paola, E. García-López, G. Marcì, L. Palmisano, A survey of photocatalytic materials for environmental remediation, J. Hazard. Mater. 211–212 (2012) 3–29.
[8] D. Jing, H. Liu, X. Zhang, L. Zhao, L. Guo, Photocatalytic hydrogen production under direct solar light in a CPC based solar reactor: Reactor design and preliminary results, Energy Convers. Manage. 50 (2009) 2919–2926.
[9] R. Portela, S. Suárez, R. Tessinari, M. Hernández-Alonso, M. Canela, B. Sánchez, Solar/lamp-irradiated tubular photoreactor for air treatment with transparent supported photocatalysts, Appl. Catal., B 105 (2011) 95–102.
[10] J.I. Ajona, A. Vidal, The use of CPC collectors for detoxification of contaminated water: Design, construction and preliminary results, Sol. Energy 68 (2000) 109–120.
[11] E.R. Bandala, C.A. Arancibia-Bulnes, S.L. Orozco, C.A. Estrada, Solar photoreactors comparison based on oxalic acid photocatalytic degradation, Sol. Energy 77 (2004) 503–512.
[12] T. Zhang, T. Oyama, A. Aoshima, H. Hidaka, J. Zhao, N. Serpone, Photooxidative N-demethylation of methylene blue in aqueous TiO_2 dispersions under UV irradiation, J. Photochem. Photobiol., A 140 (2001) 163–172.
[13] C.-H. Wu, J.-M. Chern, Kinetics of photocatalytic decomposition of methylene blue, Ind. Eng. Chem. Res. 45 (2006) 6450–6457.
[14] R. Ahmad, P.K. Mondal, Adsorption and photodegradation of methylene blue by using PAni/TiO_2 nanocomposite, J. Dispersion Sci. Technol. 33 (2012) 380–386.
[15] M. Brienza, M. Mahdi Ahmed, A. Escande, G. Plantard, L. Scrano, S. Chiron, S.A. Bufo, V. Goetz, Relevance of a photo-Fenton like technology based on peroxymonosulphate for 17β-estradiol removal from wastewater, Chem. Eng. J. 257 (2014) 191–199.
[16] P. Fernández-Ibáñez, C. Sichel, M. Polo-López, M. de Cara-García, J. Tello, Photocatalytic disinfection of natural well water contaminated by Fusarium solani using TiO_2 slurry in solar CPC photo-reactors, Catal. Today 144 (2009) 62–68.
[17] D. Alrousan, M. Polo-López, P. Dunlop, P. Fernández-Ibáñez, J. Byrne, Solar photocatalytic disinfection of water with immobilised titanium dioxide in re-circulating flow CPC reactors, Appl. Catal., B 128 (2012) 126–134.
[18] J.H. Pereira, A.C. Reis, D. Queirós, O.C. Nunes, M.T. Borges, V.P. Vilar, R.A. Boaventura, Insights into solar TiO_2-assisted photocatalytic oxidation of two antibiotics employed in aquatic animal production, oxolinic acid and oxytetracycline, Sci. Total Environ. 463–464 (2013) 274–283.
[19] G. Plantard, V. Goetz, Correlations between optical, specific surface and photocatalytic properties of media integrated in a photo-reactor, Chem. Eng. J. 252 (2014) 194–201.

[20] K.-T. Byun, H.-Y. Kwak, Degradation of methylene blue under multibubble sonoluminescence condition, J. Photochem. Photobiol., A 175 (2005) 45–50.
[21] P. Mohapatra, K. Parida, Photocatalytic activity of sulfate modified titania 3: Decolorization of methylene blue in aqueous solution, J. Mol. Catal. A: Chem. 258 (2006) 118–123.
[22] M.M. Mohamed, M.M. Al-Esaimi, Characterization, adsorption and photocatalytic activity of vanadium-doped TiO_2 and sulfated TiO_2 (rutile) catalysts: Degradation of methylene blue dye, J. Mol. Catal. A: Chem. 255 (2006) 53–61.
[23] S. Senthilkumaar, K. Porkodi, R. Gomathi, A.G. Maheswari, N. Manonmani, Sol–gel derived silver doped nanocrystalline titania catalysed photodegradation of methylene blue from aqueous solution, Dyes Pigm. 69 (2006) 22–30.
[24] S.-Y. Kim, T.-H. Lim, T.-S. Chang, C.-H. Shin, Photocatalysis of methylene blue on titanium dioxide nanoparticles synthesized by modified sol-hydrothermal process of $TiCl_4$, Catal. Lett. 117 (2007) 112–118.
[25] M.A. Abdullah, F.K. Chong, Dual-effects of adsorption and photodegradation of methylene blue by tungsten-loaded titanium dioxide, Chem. Eng. J. 158 (2010) 418–425.
[26] X. Kang, S. Chen, Photocatalytic reduction of methylene blue by TiO_2 nanotube arrays: Effects of TiO_2 crystalline phase, J. Mater. Sci. 45 (2010) 2696–2702.
[27] Y. Acosta-Silva, R. Nava, V. Hernández-Morales, S. Macías-Sánchez, M. Gómez-Herrera, B. Pawelec, Methylene blue photodegradation over titania-decorated SBA-15, Appl. Catal., B 110 (2011) 108–117.
[28] I. Boiarkina, S. Pedron, D.A. Patterson, An experimental and modelling investigation of the effect of the flow regime on the photocatalytic degradation of methylene blue on a thin film coated ultraviolet irradiated spinning disc reactor, Appl. Catal., B 110 (2011) 14–24.
[29] J. Kasanen, J. Salstela, M. Suvanto, T.T. Pakkanen, Photocatalytic degradation of methylene blue in water solution by multilayer TiO_2 coating on HDPE, Appl. Surf. Sci. 258 (2011) 1738–1743.
[30] M. Ahmed, Synthesis and structural features of mesoporous NiO/TiO_2 nanocomposites prepared by sol–gel method for photodegradation of methylene blue dye, J. Photochem. Photobiol., A 238 (2012) 63–70.
[31] C. Sahoo, A.K. Gupta, I.M. Sasidharan Pillai, Photocatalytic degradation of methylene blue dye from aqueous solution using silver ion-doped TiO_2 and its application to the degradation of real textile wastewater, J. Environ. Sci. Health., Part A, 47 (2012) 1428–1438.
[32] M. Abdelaal, R. Mohamed, Novel Pd/TiO_2 nanocomposite prepared by modified sol–gel method for photocatalytic degradation of methylene blue dye under visible light irradiation, J. Alloys Compd. 576 (2013) 201–207.
[33] D. Li, K. Xiong, Z. Yang, C. Liu, X. Feng, X. Lu, Process intensification of heterogeneous photocatalysis with static mixer: Enhanced mass transfer of reactive species, Catal. Today 175 (2011) 322–327.
[34] L.S. Roselin, G. Rajarajeswari, R. Selvin, V. Sadasivam, B. Sivasankar, K. Rengaraj, Sunlight/ZnO-mediated photocatalytic degradation of reactive red 22 using thin film flat bed flow photoreactor, Sol. Energy 73 (2002) 281–285.
[35] M. Behnajady, N. Modirshahla, N. Daneshvar, M. Rabbani, Photocatalytic degradation of an azo dye in a tubular continuous-flow photoreactor with immobilized TiO_2 on glass plates, Chem. Eng. J. 127 (2007) 167–176.
[36] D.P. Serrano, R. van Grieken, Heterogenous events in the crystallization of zeolites, J. Mater. Chem. 11 (2001) 2391–2407.
[37] A.F. Martins, M.L. Wilde, C. Da Silveira, Photocatalytic degradation of brilliant red dye and textile wastewater, J. Environ. Sci. Health., Part A 41 (2006) 675–685.
[38] D.R. Stapleton, D. Mantzavinos, M. Papadaki, Photolytic (UVC) and photocatalyic (UVC/TiO_2) decomposition of pyridines, J. Hazard. Mater. 146 (2007) 640–645.
[39] J. Bangun, A.A. Adesina, The photodegradation kinetics of aqueous sodium oxalate solution using TiO_2 catalyst, Appl. Catal., A 175 (1998) 221–235.
[40] C. Tang, V. Chen, The photocatalytic degradation of reactive black 5 using TiO_2/UV in an annular photoreactor, Water Res. 38 (2004) 2775–2781.
[41] J. Saien, A.R. Soleymani, Degradation and mineralization of Direct Blue 71 in a circulating upflow reactor by UV/TiO_2 process and employing a new method in kinetic study, J. Hazard. Mater. 144 (2007) 506–512.
[42] S. Kansal, G. Kaur, S. Singh, Studies on the photocatalytic degradation of 2,3-dichlorophenol using different oxidants in aqueous solutions, React. Kinet. Catal. Lett. 98 (2009) 177–186.
[43] M.L. Satuf, R.J. Brandi, A.E. Cassano, O.M. Alfano, Quantum efficiencies of 4-chlorophenol photocatalytic degradation and mineralization in a well-mixed slurry reactor, Ind. Eng. Chem. Res. 46 (2006) 43–51.
[44] B. Bayarri, E. Carbonell, J. Gimenez, S. Esplugas, H. Garcia, Higher intrinsic photocatalytic efficiency of 2,4,6-triphenylpyrylium-based photocatalysts compared to TiO_2 P-25 for the degradation of 2,4-dichlorophenol using solar simulated light, Chemosphere 72 (2008) 67–74.
[45] M. Karkmaz, E. Puzenat, C. Guillard, J.M. Herrmann, Photocatalytic degradation of the alimentary azo dye amaranth, Appl. Catal., B 51 (2004) 183–194.
[46] H. Jiang, G. Zhang, T. Huang, J. Chen, Q. Wang, Q. Meng, Photocatalytic membrane reactor for degradation of acid red B wastewater, Chem. Eng. J. 156 (2010) 571–577.
[47] Z. Yigit, H. Inan, A study of the photocatalytic oxidation of humic acid on anatase and mixed-phase anatase–rutile TiO_2 nanoparticles, Water Air Soil Pollut. Focus 9 (2009) 237–243.